Journal of Population Therapeutics & Clinical Pharmacology

Guazuma tomentosa and *Abutilon indicum* - A Novel Mixed green inhibitor for acid corrosion of aluminum alloy

[a]Anusha B, Associate Professor, Department of Physics, Sri Sairam Institute of Technology,
[b]Rajabhuvaneswari Ariyamuthu, Professor, Department of Chemistry, Bharath Institute of Higher Education and Research, Seliyur, Chennai -600073.
[c]Jeevalatha Rugmangathan, Assistant Professor, Department of Chemistry, Panimalar Engineering College, Chennai City Campus, Chennai-600029, Tamilnadu, India.
[d]Balamurugan Arumugam, Assistant professor, Research Department of Chemistry, Thiagarajar College, Madurai-625009, Tamilnadu, India.
Corresponding Author E-mail: jeevalathar@gmail.com

Abstract
The study of ethanolic extract of corrosion inhibition on the aluminum alloy in 1M HCl and 1M H_3PO_4 by a mixed inhibitor (GTLE +AILE) has been studied at different temperatures viz., 303, 308, 313, 318, 323 K by gravimetric method and electrochemical measurement. The inhibition efficiency increases with increasing concentration of inhibitor and decreases with the rise in temperature of both the acid media. The potentiodynamic polarization study confirmed that the inhibitor acts as a mixed type of inhibitor, controlling the anodic and cathodic corrosion reactions. The inhibitive action of the extract revealed that, the adsorption of mixed inhibitor on aluminium alloy follows physisorption mechanism. The adsorptive behaviour of the active constituents was carried out by UV-visible, FT-IR spectroscopic studies. Surface morphology was examined by using scanning electron microscopy (SEM) which was confirmed the existence of a protective film of mixed inhibitor molecule on the aluminium alloy surface.

Keywords: Corrosion inhibition, mixed inhibitor, Aluminium alloy, structural analysis.

1 Introduction

All industries must deal with corrosion, which is one of the worst technological disasters in human history. Owing to their numerous industrial requirements and financial deliberations, corrosion studies of aluminium and their corresponding alloys have drawn significant environmental attention [1–3]. Due to the growing awareness it is in the need to protect the world's metal resources, corrosion studies have also become crucial [4]. In the fields of aerospace, automotive, construction, electrical power generation, and some chemical processing, aluminium and its alloys have become substitute materials. Due to their numerous uses, metals frequently come into contact with acids or

bases during processes like pickling, de-scaling, and electrochemical etching [5, 6]. The accumulation of organic or inorganic compounds to the suspension that is in direct interaction with the surface, to prevent the corrosion reaction and decrease their rate, is a useful technique for preventing corrosion in metals and alloys used in aggressive environments. It is known that several organic compounds [7–10] can be used to prevent the corrosion of aluminium alloy (AA) in acidic atmospheres. Those substances that are part of a conjugated system and contain oxygen, nitrogen, or sulphur may be adsorbed on the metal surface as a result of corrosion, forming a barrier layer. The bond strength, metal composition, type of corrodant, inhibitor concentration, and temperature all affect how well molecules adhere to surfaces. In India, well-known and widely accessible plants include *Guazuma tomentosa* and *Abutilon Indicum*. Their corresponding leaf extracts are denoted as (GTLE and AILE). AILE and GTLE are members of the Malvaceae family, which also includes many compounds like sterculiaceae. Colistin, catechins, caffeine, kaempferol, procyanidins, tartaric acid, and xanthan gum are among the phytochemical components of GTLE, while the AILE extract contains sugars, steroids, alkaloids, amino acids, fatty acids, flavonoids, and tannins [11, 12]. Past studies on the mixed inhibitor (GTLE and AILE) and their ability to prevent the corrosion of the AA in HCl and H_3PO_4 have not been published in the literature. At this point, it has been decided to use extracts of *Guazuma tomentosa* and *Abutilon indicum* for the first time as mixed inhibitors in the current work to reduce the corrosion of AA in HCl and H_3PO_4 to the greatest extent possible. The corresponding gravimetric, adsorption isotherm, electrochemical, structural and morphological analysis were achieved by using various techniques, including FT-IR, SEM, EDAX, and electrochemical measurements. From the observed results we concluded that the mixed inhibitor (GTLE + AILE) is the outstanding candidate for corrosion inhibition studies in AA.

2 Experimental

2.1 Preparation of the Specimen

The AA specimen (Al = 71.55 %, O = 41.68 %, C = 8.72 %, Si = 1.31%, Cl = 1.27 %) of dimensions size 2.5 x 2.5 x 0.4 cm was used for the current study. The AA specimens were polished with emery paper of 4/0 grade. All specimens were thoroughly cleaned with absolute ethanol, dehydrated at room temperature, and stored in a desiccator without moisture. All the chemicals and substances used in this study were of analytical grade. 1M HCl and 1M H_3PO_4 were used as corrosive solution.

2.2 Preparation of the leaf extract

Guazuma tomentosa and *Abutilon Indicum* leaves were collected and then the leaves were cut into small pieces, allowed to dry for seven days in the shade, and then ground into a fine powder. Absolute ethanol was used to extract 10g of each dried powder over the course of 5 hours in the soxhlet apparatus. The extract was filtered off after extraction was finished, and the residue was then obtained by heating the extract on a water bath at 100 ^{o}C. From the stock residue, seven inhibitor sample suspensions with the concentration of 0, 10, 20, 30, 40, 50 and 100 mg/100 mL were prepared.

2.3 Gravimetric experiment

The pre-weighed AA specimens were immersed in 100 mL of the above test solutions and each set of samples was maintained at different temperatures of 303, 308, 313, 318 and 323 K for 3 h. After the specified immersion period, the specimens were removed, rinsed with water and ethanol, dried and stored in a desiccator. The dried specimens were weighed again and the weight loss were determined. The corrosion rate (CR) (ƛ) and the percentage of inhibition efficiency (IE %) was calculated using the following equations 1 and 2 [13].

$$\eta\% = \frac{W_o - W_i}{W_o} X\ 100 \qquad (1)$$

$$C_R = \frac{87.6\ X\ W}{A\ X\ T\ X\ D} \qquad (2)$$

Where the exposure time denoted as T expressed in hours (h). A stand for specimen's area in cm^2, W for weight loss, D for the AA density in g/cm^3, and W_0 and W_i for weight loss in the presence and absence of inhibitors, correspondingly.

2.4 Electrochemical Measurement

An electrochemical workstation - CHI760D equipped with three electrode system were utilized to analyze the electrochemical parameters such as Nyquist impedance curve and Tafel polarisation curve. Three electrode system consisting of the AA specimen with an exposed area size of 0.5 cm^2 as a working electrode, Platinum electrode as counter electrode and saturated calomel as reference electrodes respectively. The AA specimen was immersed in different sample solutions. The experiments were carried out at 303 K with 100 mL of electrolyte (1M HCl and 1M H_3PO_4) in a stationary condition. The electrode was allowed to corrode and its open circuit potential (OCPT) was measured, before each measurement of potentiodynamic polarization (Tafel) and electrochemical impedance spectroscopy (EIS) were carried out. Potentiodynamic polarization curves were recorded from -250 to +250 mv SCE, (versus OCPT) with a scan rate of 0.01 vs^{-1}. The real part and imaginary part of the cell impedance were measured in ohms for various frequencies. The double-layer capacitance (C_{dl}) and charge-transfer resistance (R_{ct}) values were calculated using the following equation (3) and (4) [14].

$$R_{ct} = (R_s + R_{ct}) - R_s \qquad (3)$$

$$C_{dl} = {}^{1}/_{2\pi R_{ct} f_{\max}} \qquad (4)$$

3. Surface Analysis

3.1 Fourier Transform-Infra Red spectroscopy (FT-IR)

The functional groups present in the specimen were characterized using FT-IR spectroscopy (Bruker Instruments). The specimen used here was immersed in 100 mL of an acid solution containing the optimum concentration of inhibitor for 24 hrs. Later a specified immersion period, the specimen was taken out, dried, and then formed into a disc by being rubbed with a small amount of KBr powder [14]. FT-IR spectra were recorded. The above procedure was performed for the mixed inhibitor (GTLE + AILE) residue.

3.2 Scanning Electron Microscopy and EDAX analysis

In both the absence and presence of the ideal concentration of inhibitor, the AA specimen was submerged in an acid solution for 24 hours. Later the specific immersion period, the specimen was taken out, dried and SEM and EDAX characterization were carried out using Bruker Scanning Electron Microscopy and EDAX Spectrometer.

4 Results and Discussion

4.1. Gravimetric experiment

The rate of corrosion of an AA in 1M HCl in the presence and absence of various combination inhibitor doses (GTLE + AILE) leaf extracts was determined at 303 – 323K as shown in **Table 1. Figure 1 (A, C)** demonstrates the effect of the concentration of mixed inhibitor (GTLE + AILE) on the inhibition efficiency (IE) and corrosion rate (CR) of AA in 1M HCl in the blank and various concentrations of mixed inhibitor (GTLE + AILE) extract.

Table 1. Variation of Corrosion rate (CR) and Inhibition efficiency (IE) of mixed inhibitor (GTLE + AILE) on AA corrosion as a function of temperature in 1M HCl

***Mixed inhibitor Residue* (mg)**	**303K**		**308K**		**313K**		**318K**		**323K**	
	CR (mpy)	**IE %**	**CR (mpy)**	**IE %**	**CR (mpy)**	**IE %**	**CR (mpy)**	**IE %**	**CR (mpy)**	**IE %**
0	0.4934	-	0.4462	-	0.4147	-	0.3832	-	0.3377	-
10	0.1172	76.24	0.1207	72.94	0.1277	69.19	0.1364	64.38	0.1487	55.95
20	0.0962	80.49	0.1014	77.25	0.1137	72.57	0.1207	68.49	0.1294	61.65
30	0.0752	84.75	0.0822	81.56	0.0979	76.37	0.1067	72.14	0.1207	64.24
40	0.0542	89	0.0612	86.27	0.0717	82.7	0.0822	78.53	0.0927	72.53
50	0.0332	93.26	0.0437	90.19	0.0594	85.65	0.0664	82.64	0.0804	76.16
100	0.0139	97.16	0.0332	92.54	0.0437	89.45	0.0507	86.75	0.0664	80.13

Figure 1 (C) shows that the rate of AA corrosion slowed down as the inhibitor's concentration increased, indicating that the mixed inhibitor leaf extract (GTLE + AILE) in 1M HCl was effective in preventing AA corrosion. The amount of the extract present in 1M HCl determines how much corrosion was inhibited by the extract. **Figure 1 (A)** reveals that IE of AA upsurges while increase in the inhibitor concentration. The IE was maximum in that is 97 % for 100 mg/100 mL of HCl, which indicates that the mixed inhibitor (GTLE + AILE) was the best inhibitor for 1M HCl.

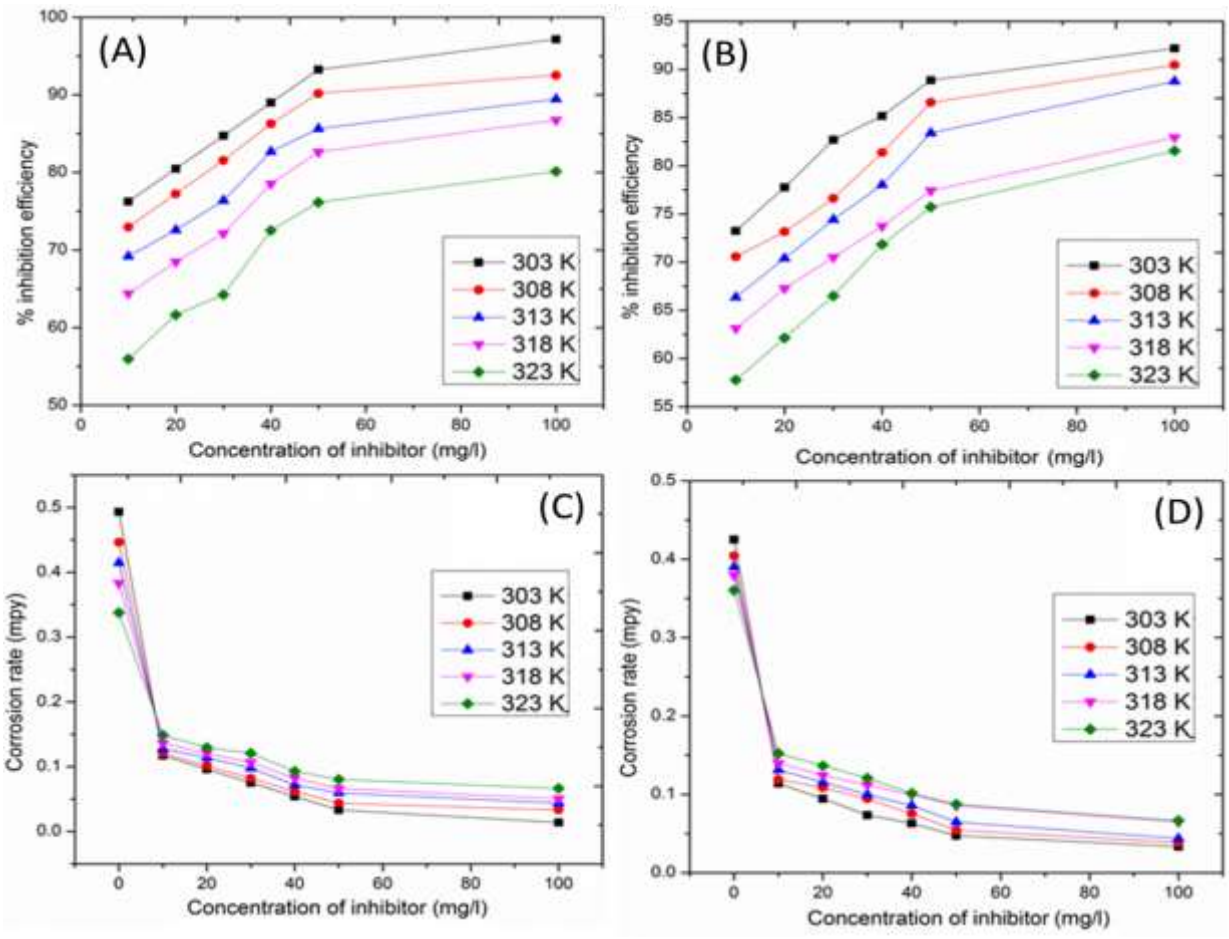

Figure 1 (A, B) Variation of inhibition efficiency (IE) and **(C, D)** variation of corrosion rate (CR) of AA in 1M HCl and 1M H_3PO_4 in with and without mixed inhibitor (GTLE + AILE).

Figure 2 (A) which is the corresponding plot for IE in contradiction of different temperatures, for different mixed inhibitor (GTLE + AILE) concentration of specimens, show that the desorption of mixed inhibitor (GTLE + AILE) caused the inhibitor efficiency to decrease as the temperature increases from the surface of AA [15,16]. **Figure 2 (C)** which is the plot for difference in CR against time for different mixed inhibitor (GTLE + AILE) concentrations against specimens indicates CR of the AA decreases with an increase in the period of contact time for blank and inhibitor acid solution.

Table 2. Variation of CR and IE of mixed inhibitor (GTLE + AILE) on AA corrosion as a function of temperature in 1M H_3PO_4

***Mixed inhibiton Residue* (mg)**	**303K**		**308K**		**313K**		**318K**		**323K**	
	CR (mpy)	**IE %**	**CR (mpy)**	**IE %**	**CR (mpy)**	**IE %**	**CR (mpy)**	**IE %**	**CR (mpy)**	**IE %**
0	0.4252	-	0.4042	-	0.3902	-	0.3797	-	0.3604	-
10	0.1137	73.25	0.1189	70.56	0.1312	66.36	0.1399	63.13	0.1522	57.76

20	0.0944	77.77	0.1084	73.16	0.1154	70.4	0.1242	67.28	0.1364	62.13
30	0.0734	82.7	0.0944	76.62	0.0997	74.43	0.1119	70.5	0.1207	66.5
40	0.0629	85.18	0.0752	81.38	0.0857	78.02	0.0997	73.73	0.1014	71.84
50	0.0472	88.88	0.0542	86.58	0.0647	83.4	0.0857	77.41	0.0874	75.72
100	0.0332	92.18	0.0384	90.47	0.0437	88.78	0.0647	82.94	0.0664	81.55

The long immersion time may have reduced the amount of inhibitor molecules that were present in the solution, which was caused by the complex that formed between the inhibitor molecules and the AA. The CR of AA in 1M H_3PO_4 with and without presence of different mixed inhibitor (GTLE + AILE) leaf extracts concentrations were determined at 303–333K as shown in **Table 2. Figure 1 (B, D)** demonstrates the influence inhibitor concentrations on the IE and CR of AA in 1M H_3PO_4 in the blank and various concentration. From **Figure 1 (B)** reveals that the IE of the AA increases with an increase in the concentration of the inhibitor. The IE maximum is observed to be 92 % for 100mg/100mL of H_3PO_4, which indicates that the mixed inhibitor (GTLE + AILE) was the best inhibitor for 1M H_3PO_4. **Figure 1 (D),** clears that the rate of corrosion of AA decreases while with increasing inhibitor concentration which approves that the corrosion of AA was inhibited by mixed inhibitor (GTLE + AILE) leaf extract in 1M H_3PO_4 and the amount of corrosion inhibition is being subject to the amount of extract present in 1M H_3PO_4.

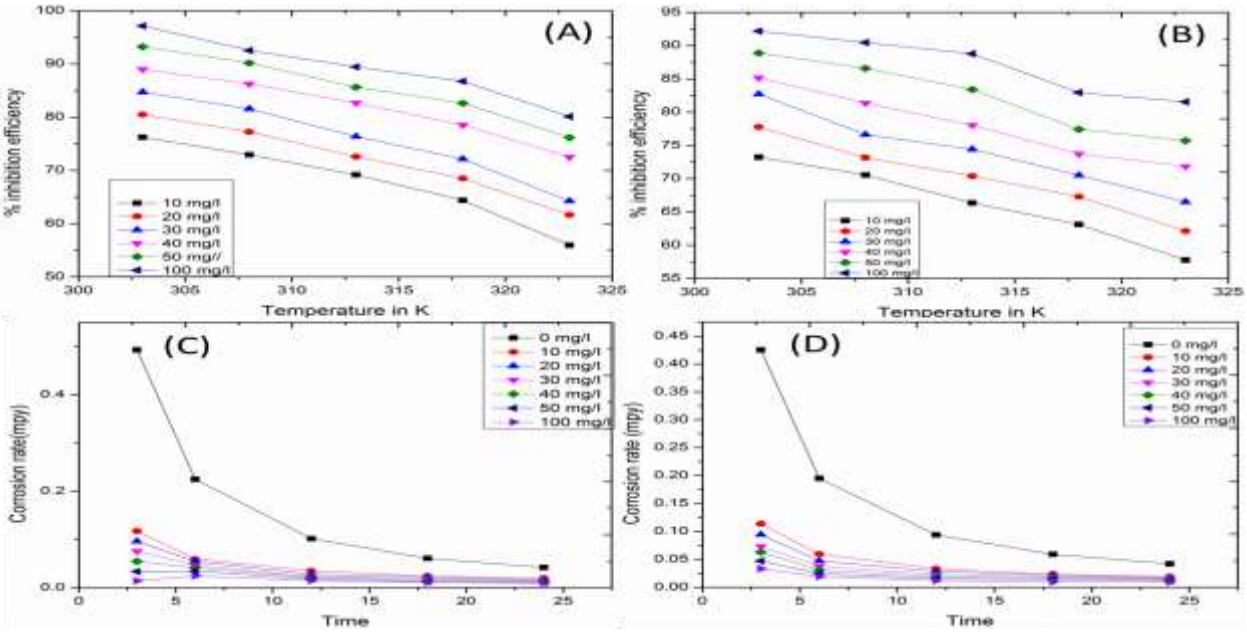

Figure 2 (A, B) Variation of IE vs. temperature when mixed inhibitor (GTLE + AILE) concentrations are varied (in 1M HCl and 1M H_3PO_4), **(C, D)** Time-dependent CR of a combined inhibitor (GTLE+ AILE) in 1M HCl and 1M H_3PO_4.

Figure 2 (B) demonstrate the plot of IE vs. different temperatures, for different mixed inhibitor (GTLE + AILE) concentration of specimens indicate that when temperature rose, the effectiveness of the inhibitor diminished as a result of the mixed inhibitor's (GTLE + AILE) desorption from the

surface of the AA. **Figure 2 (D)** which is the plot for variation of CR against time for different mixed inhibitor (GTLE + AILE) concentration indicates CR of the AA decreases with an increase in the period of contact time for blank and inhibitor acid solution. The decrease in IE is due to the long period of immersion and may be attributed to the depletion of available inhibitor molecules in the solution which is due to the formation of the complex between AA and the inhibitor molecules. From the above results, it was concluded that the IE for the inhibitor in 1M HCl is greater than that of (97 %) compared to 1M H_3PO_4 which is 92 %.

4.2. Adsorption isotherm consideration

Adsorption isotherms provide information about the interaction between the inhibitor and AA surface. The values of surface coverage (θ) were applied to various adsorption isotherm models including Langmuir, Freundlich and Tempkin to detect the magnitude of adsorption. The mixed inhibitor (GTLE + AILE) in 1M HCl obeys the Langmuir adsorption isotherm model [14].

$$\frac{C}{\theta} = \frac{1}{K_{(ads)}} + C \qquad (5)$$

Where, concentration of mixed inhibitor (in mg/l) represented as C, adsorption-desorption equilibrium constant denoted as K, surface coverage represented as θ [21]. **Figure 3 (A, B)** displays the plot of C against C/θ for mixed inhibitor (GTLE + AILE) extracts at 30–50 ºC. Linear plots were obtained and the adsorption parameters derived from the plot and the R^2, $-\Delta G^o_{ads}$, K, ΔH^o_{ads}, $-\Delta S^o_{ads}$ values are listed in **Table 3.** The R^2 values which are greater than 0.9 indicate that the system obeys Langmuir adsorption isotherm. The K_{ads} morals specify the binding efficiency of the inhibitor to the metal surface, are seems to decrease with increasing temperature in both the acids ((a) 1M HCl, (b) 1M H_3PO_4) and it may be attributed to the interaction between the adsorbed molecules and the metal surface which is too weak [14]. The adsorption of inhibitor molecules is well-explained by the thermodynamic model.

Table 3. Langmuir adsorption characteristics and free energy of adsorption of mixed inhibitor (GTLE + AILE) on the surface of AA in (a) 1M HCL (b) 1M H_3PO_4

Temp (K)	$-\Delta G^o_{ads}$		K		$-\Delta H^o_{ads}$ (kJ mol^{-1})		ΔS^o_{ads} (J mol k^{-1})		R^2	
	a	b	a	b	a	b	a	b	a	b
303	6.39	6.38	2.2	2.2	5.91 x 10^{-4}	5.77 x 10^{-4}	20.77	21.07	0.99	0.99
308	6.19	5.76	2.1	1.7	6.07 x 10^{-4}	6.88 x 10^{-4}	20.43	18.72	0.99	0.99
313	5.97	5.57	1.7	1.4	6.61 x 10^{-4}	7.20 x 10^{-4}	19.07	17.54	0.99	0.99
318	5.54	5.45	1.4	1.4	7.25 x 10^{-4}	7.38 x 10^{-4}	17.43	17,41	0.99	0.99
323	5.01	4.99	1.1	1.1	7.94 x 10^{-4}	7.97 x 10^{-4}	15.53	15.47	0.99	0.99

The Van't Hoff equation could be used to calculate the enthalpy of adsorption [8, 22].

$$lnK_{ads} = \frac{-\Delta H^{o}_{ads}}{RT} + constant \qquad (6)$$

The straight lines of the plot of lnK versus 1/T are shown in **Figure 3 (C, D),** and their slope is equal to $-H_{ads}/R$. According to the adsorption's free energy values, only physical adsorption is responsible for the inhibitors' adhesion to the metal surface. Free energy of adsorption values up to -20 kJ mol^{-1} typically correspond to electrostatic interaction between charged molecules and a charged metal (which indicates physical adsorption) [19, 23-25]. The values of ΔG_{ads} specifies that the adsorption mechanism of mixed inhibitor (GTLE + AILE) on AA in both the acids (HCl and H_3PO_4) solution is typical of physisorption's [13, 26].

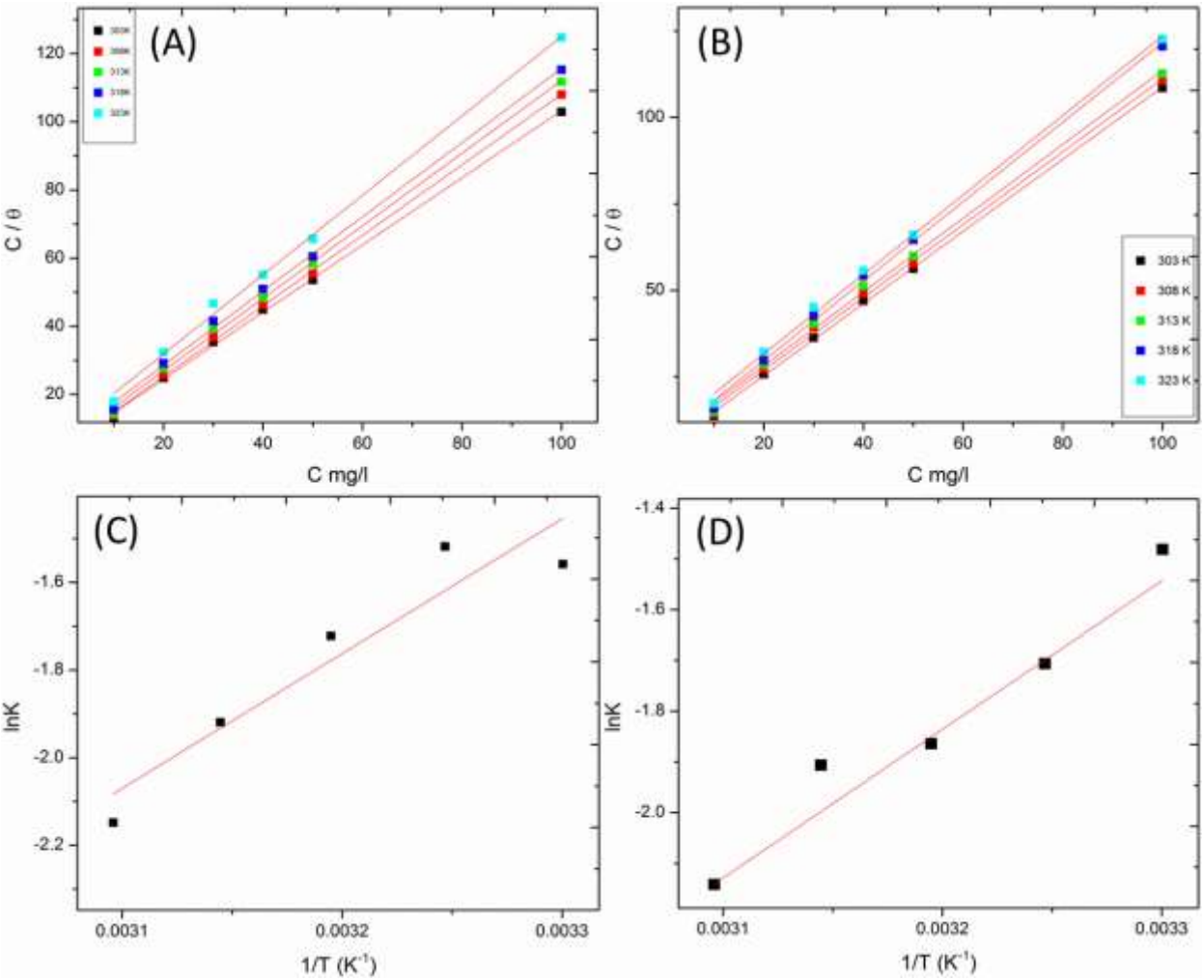

Figure 3 (A, B) Langmuir adsorption isotherm plots for AA in 1M HCl and 1M H_3PO_4 with mixed inhibitor (GTLE+ AILE) extract at different temperatures, **(C, D)** Plots of lnK vs. 1/T for the adsorption of mixed inhibitor (GTLE + AILE) of AA / HCL interface and H_3PO_4 interface.

The following equation relates the equilibrium constant (K) to the standard free energy of adsorption (G_{ads}) [13].

$$\Delta G = -RTln\,(55.5K) \qquad (7)$$

Where R is the gas constant, T is the temperature and 55.5 is the molar concentration of water in the solution. Under experimental circumstances, the heat of adsorption might roughly be regarded as the standard heat of adsorption (ΔH_{ads}). The following equation yields the standard adsorption entropy (ΔS_{ads}) [27].

$$\Delta S_{ads} = \frac{\Delta H_{ads} - \Delta G_{ads}}{T} \qquad (8)$$

The results show that the values of H_{ads} are negative, indicating that the inhibitor is adsorbing through an exothermic process, which means that the dissolution of the AA was slow in the presence of the inhibitor [28]. The values of ΔS_{ads} are positive at a temperature range of 303 – 333K and the positive entropy values (ΔS*) suggest that the activated complex represents a dissociation step rather than an association step in the rate-determining step, which means that the disorder decreases as one moves from reactants to the activated complex [13,22,29]. The above study was carried out using 1M H_3PO_4 instead of 1M HCl. As shown in **Figure 3 (B),** the mixed inhibitor (GTLE+ AILE) in 1M H_3PO_4 follows the Langmuir adsorption isotherm by providing a straight line for the plot of C vs. C/ θ.

4.3. Thermodynamic parameters for inhibition process

The activation conditions for the corrosion process were calibrated using the Arrhenius Equation (9) and the Transition State Equation (10) [13].

$$C_R = A_{exp}\left(\frac{-E_a}{RT}\right) \qquad (9)$$

$$C_R = \frac{RT}{hN}\exp\left(\frac{\Delta S^*}{R}\right)\exp\left(\frac{-\Delta H^*}{RT}\right) \qquad (10)$$

Where T is the absolute temperature, A denotes the frequency factor, Ea represents the activation energy, R signifies the gas constant (R = 8.314 J mol^{-1} K^{-1}), h denotes the Planck constant, and N is Avogadro's number. A calibration plot of log CR vs. 1/T displayed in **Figure 4 (A, B)** and log CR/T vs. 1/T were displayed in **Figure 4 (C, D)** gave Arrhenius and transition state linear fitting plots with a slope of (-Ea/2.303R) and (-H*/2.303R), respectively. The corresponding intercept will be A and [(log R/hN + (S*/2.303R)], respectively. The calculated values of apparent activation energy (E_a), activation entropies (ΔS*) and activation enthalpies (ΔH*) are listed in **Table 4.** The increase in the values of E_a from 9.70 to 58.13 kJ mol^{-1} (1M HCl) and 6.4 to 31.04 kJ mol^{-1} (1M H_3PO_4,), specifies the higher IE of the inhibitor which is due to the adsorption of inhibitor molecules on the metal surface to form the stable metal-inhibitor complex.

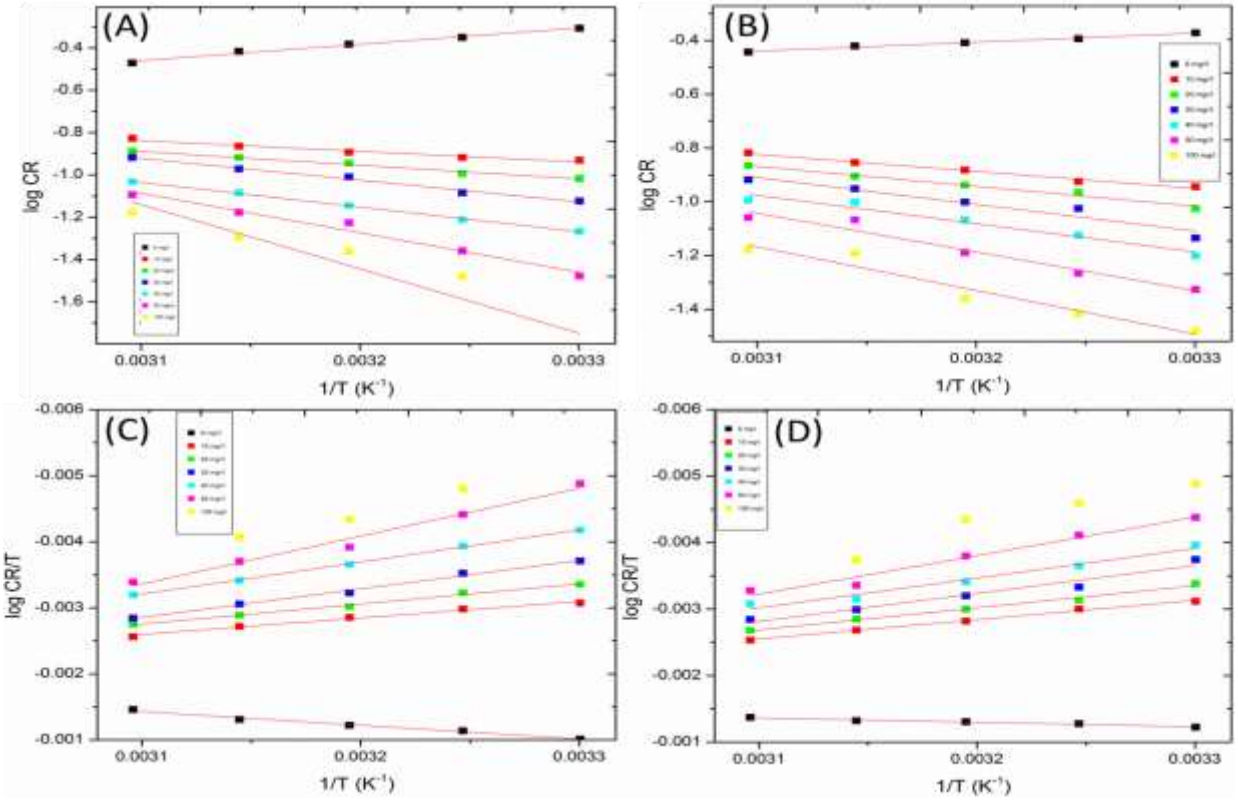

Table 4. Corrosion kinetic parameters of aluminium alloy in (a) 1M HCL (b) 1M H_3PO_4 with and without presence of different mixed inhibitor (GTLE + AILE) concentrations

C_{inh} (mg)	$-E_a$ (kJ mol^{-1})		$-\Delta H^*$(kJ mol^{-1})		$-\Delta S^*$(J $molk^{-1}$)	
	a	b	a	b	a	b
0	9.70	6.4	39.92	12.67	197.58	197.57
10	12.48	12.12	47.92	55.68	197.56	197.56
20	14.80	14.21	58.20	63.52	197.56	197.56
30	19.64	19.03	82.43	80.38	197.55	197.55
40	22.27	20.20	93.25	85.52	197.55	197.55
50	35.68	27.54	138.73	110.81	197.55	197.55
100	58.13	31.04	271.45	271.54	197.54	197.54

The negative values of enthalpies (ΔH*), ranged from 39.92 to 271.45 kJ mol^{-1} (1M HCl) and 12.67 to 271.54 (1M H_3PO_4), showing that the process is endothermic and it needs more energy to achieve the activated state or equilibrium [30]. The activated complex in the rate-determining step is implied to be due to an association rather than a dissociation by the negative values of entropy (ΔS*), which means that the disorder decreases as one moves from reactants to the activated complex [23, 31, 32]. From the results of 1M HCl and 1M H_3PO_4, it was concluded, for both cases the energy of activation increases to the increasing concentration.

Figure 4 (A, B) Arrhenius plots and **(C, D)** Transition state plots for AA in 1M HCl and 1M H_3PO_4 with and without presence of various concentration of mixed inhibitor (GTLE + AILE).

4.4. Electrochemical measurement

4.4.1. Potentiodynamic polarization studies

Polarization study is one of the methods for the confirmation of the formation of a protective film on the metal surface during the corrosion inhibition process. The polarization curves of AA in 1M HCl solution for the blank and different concentrations of inhibitor solutions are displayed in **Figure 5 (A). Table 5** lists the electrochemical kinetic parameters that were derived [17] from Tafel curves, including corrosion potential (E_{corr}), cathodic and anodic slope (b_c and b_a), corrosion current density (i_{corr}), and % of IE. In this present work, the maximum shift of E_{corr} values is in the range of 39 mV which confirms that the mixed inhibitor (GTLE + AILE) acts as a mixed-type of inhibitor [13]. The IE % was calculated by using the following equation (11).

$$IE\% = \left(i^{o}_{corr} - \frac{i_{corr}}{i^{o}_{corr}}\right) X\ 100 \qquad (11)$$

Where, i_{corr} and i^{o}_{corr} are the density of corrosion current values for blank and inhibitor specimens respectively.

Table 5. Potentiodynamic polarization parameters for the corrosion of AA in (a) 1M HCl and (b) 1M H_3PO_4 containing different concentrations of mixed inhibitor (GTLE + AILE)

Mixed Inhibitor Residue *(mg)*	E_{corr} *(mV)*		I_{corr} *mA cm^{-2}*		$-b_c$ *(mV dec^{-1})*		$-b_a$ *(mV de^{-1})*		R_p (Ω cm^2)		IE *(%)*	
	a	b	a	b	a	b	a	b	a	b	a	b
0	-295	-400	297	332.5	7.39	6.92	3.82	3.77	271.3	313.4	-	-
10	-333	-408	115.1	157.3	7.11	6.84	3.79	3.62	107.1	147.1	61.2	52.7
20	-446	-426	76.3	124.4	6.96	6.57	3.71	3.53	72.5	124.6	74.3	62.5
30	-455	-449	55.2	95.7	6.87	6.02	3.65	3.39	53.2	101.5	81.4	71.2
40	-543	-595	24.6	73.1	6.82	5.91	3.43	3.27	24.7	79.8	91.7	78
50	-593	-409	19.2	42.5	6.72	5.73	3.32	3.13	19.8	48.3	93.5	87.2
100	-584	-479	15.3	25.3	6.62	5.44	3.27	3.08	16	29.5	94.8	92.4

Table 5 exhibits that i_{corr} decreases in the presence of mixed inhibitor (GTLE + AILE) than the blank solution which was due to the increases in the blocked fraction of electrode surface by adsorption. The above values contain the formation of the protective layer on the metal surface. The anodic reaction was more tightly controlled than the cathodic one at all concentrations, as evidenced by the values of b_a being lower than those of b_c [12]. In addition, the polarization curves of AA in 1M H_3PO_4 solution for the blank and various concentrations of inhibitor solutions are shown in **Figure 5 (B)** and the corresponding electrochemical kinetic parameters are given in

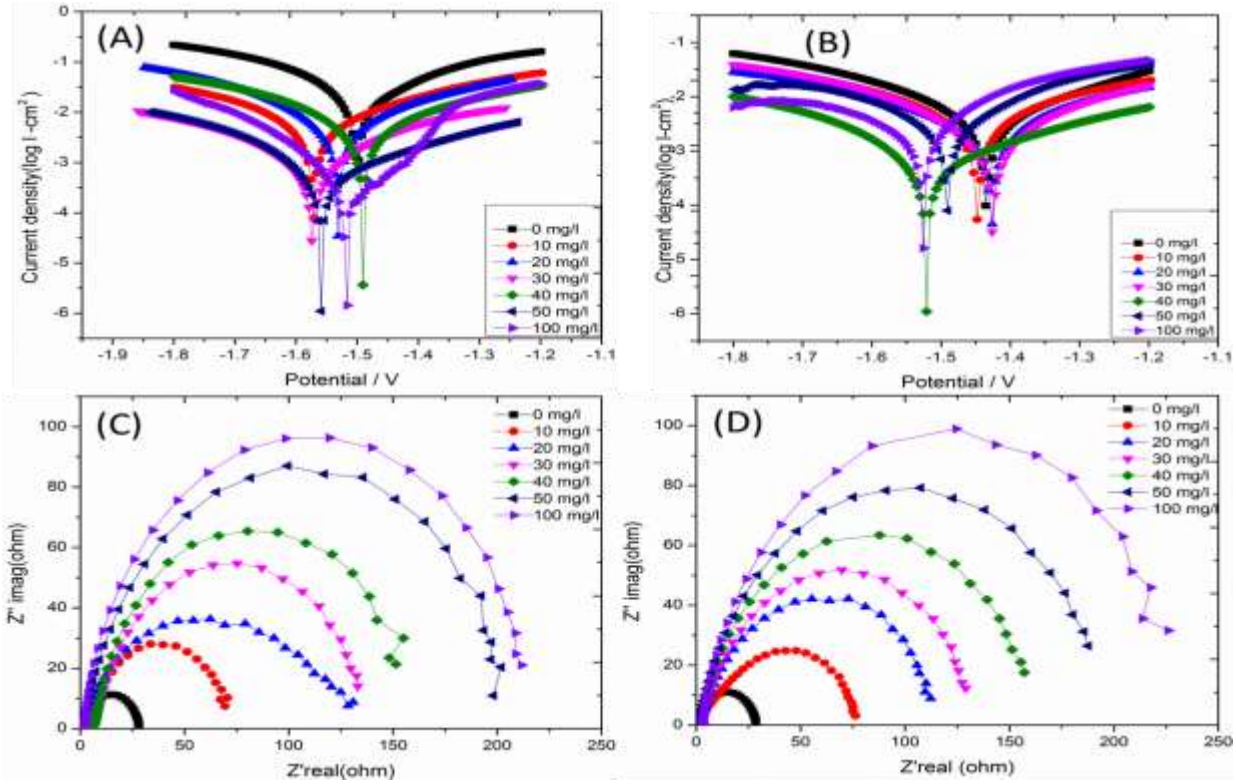

Table 5. In this present work the extreme shift E_{corr} values are in between 8 mV which confirms that the mixed inhibitor (GTLE + AILE) acts as a mixed-type of inhibitor. **Table 5** shows that i_{corr} decreases in the presence of mixed inhibitor (GTLE + AILE) than the blank solution owing to the increases in the congested portion of electrode surface by adsorption. The above values contain the formation of the protective layer on the metal surface. The values of b_a are less than that of b_c which suggests that the anodic reaction was more controlled than the cathodic one at all concentrations. From the results it has been concluded that for both acids the I_{corr} values are decreases with the increase in the inhibitor concentration which indicates that there is a formation of a protective film by the inhibitor molecules.

4.4.2 Electrochemical impedance measurement

Nyquist plots for AA in 1M HCl in the presence and absence of the various concentration of mixed inhibitor (GTLE + AILE) inhibitors are shown in **Figure 5 (C).** The impedance parameters such as R_s, R_{ct}, C_{dl} and f_{max} derived from Nyquist plots are given in **Table 6.** The percentage of IE was calculated using the following equation [18]

$$IE\% = (R_{ct(inh)-} R_{ct} / R_{ct(inh)} X\ 100 \qquad (12)$$

Figure 5. (A, B) Potentiodynamic polarisation curves of AA in 1M HCl and 1M H_3PO_4 with and without concentration of mixed inhibitor (GTLE + AILE) at 303K, **(C, D)** Nyquist plots for AA in 1M HCl and 1M H_3PO_4 with and without mixed inhibitor (GTLE + AILE) at 303K

The charge-transfer resistance increases with an increase in the concentration of mixed inhibitor (GTLE + AILE) in an acid solution, which indicates the formation of the protective adsorption layer. From **Table 6**, it is clear that as the concentration of mixed inhibitor (GTLE + AILE) increases, both the charge transfer resistance value (R_{ct}) and percentage of IE also increases which confirms the formation of a protective layer on the metal surface [19,20]. The double layer capacitance (C_{dl}) decreases with the increase in the concentration of mixed inhibitor (GTLE + AILE). From **Table 6**, it is clear that double-layer capacitance (C_{dl}) decreases and the percentage of IE increases. The diameter of the Nyquist plot increases with an increase in the concentration of the mixed inhibitor (GTLE + AILE) which indicates the adsorption of the inhibitor molecules on the metal surface. Charge transfer resistance value (R_{ct}), double layer capacitance (C_{dl}), and the increase in the diameter of the Nyquist plot confirms the formation of the protective layer on the AA surface [13]. In addition to that the Nyquist plots for AA in 1M H_3PO_4 in the presence and absence of the various concentration of mixed inhibitor (GTLE + AILE) are shown in **Figure 5 (D).** The impedance parameters such as R_s, R_{ct}, C_{dl}, and f_{max} derived from Nyquist plots are given in **Table 6.** The charge-transfer resistance increases with an increase in the concentration of mixed inhibitor (GTLE + AILE) in an acid solution, which indicates the formation of the protective adsorption layer.

Table 6. Electrochemical impedance studies for AA in (a) 1M HCl & (b) 1M H_3PO_4 in the absence and presence of mixed inhibitor (GTLE + AILE)

Mixed Inhibitor Residue (mg)	R_{ct} (Ω cm^2)		C_{dl} (µF cm^{-2})		% IE	
	a	b	a	b	a	b
0	27.2	28.3	487	473	-	-
10	70.6	76.2	115	109	61.4	62.8
20	124.9	109.6	93	98	78.2	74.1
30	132.6	127.3	81	87	79.4	77.7
40	155	155.4	72	75	82.4	81.7
50	201.9	185.5	67	62	86.5	84.7
100	228.9	213.6	58	56	88.1	86.7

From **Table 6**, it is clear that as the concentration of mixed inhibitor (GTLE + AILE) increases, both the charge transfer resistance value (R_{ct}) and the percentage of IE also increases which confirms the formation of a protective layer on the metal surface. The double layer capacitance (C_{dl}) decreases with the increase in the concentration of mixed inhibitor (GTLE + AILE). From **Table 6**, it is clear that double layer capacitance (C_{dl}) decreases and percentage of IE increases. The diameter of the Nyquist plots increases with an increase in the concentration of the mixed inhibitor (GTLE + AILE) which indicates the adsorption of the inhibitor molecules on the metal surface. The results were listed in **Table. 6** [charge transfer resistance (R_{ct}) and double layer capacitance (C_{dl})]

and the increase in the diameter of the Nyquist plots, confirms the formation of the protective layer on the AA surface.

4.5. Surface Analysis

4.5.1. FT-IR Studies

The FT-IR Spectrum of mixed inhibitor (GTLE + AILE) leaf extract is shown in **Figure 6 (A)** curve (a), The FT-IR spectrum of adsorbed protective layer formed on an AA surface after immersion in acid containing 100mg/100mL of mixed inhibitor (GTLE + AILE) is shown in **Figure 6 (A)** curve (b). In **Figure 6 (A)** curves (a) and (b) the band at 3493 cm^{-1} was found at O-H stretching vibration and the N-H stretch at 3390 cm^{-1} was shifted to 3400 cm^{-1} indicates that there is an interaction between the mixed inhibitor and the AA surface. The peak at 2400 cm^{-1} is due to the C = N stretching vibration. The band at ≈ 400 cm^{-1} is due to the presence of some halogen compounds. The result confirmed the complete coordination between metal and the inhibitor complex on the surface of AA [4].

4.5.2. EDAX Analysis

Figure 6 (B) represents the EDAX spectrum of the corroded sample of inhibited AA. **Table 7** gives the EDAX analysis result of AA in 1.0M HCl acid solution with and without presence of mixed inhibitor (GTLE + AILE) inhibitors. The spectrum reveals that the rise in the amount of oxygen is due to the existence of aluminium hydroxide film on the surface of the metal [5].

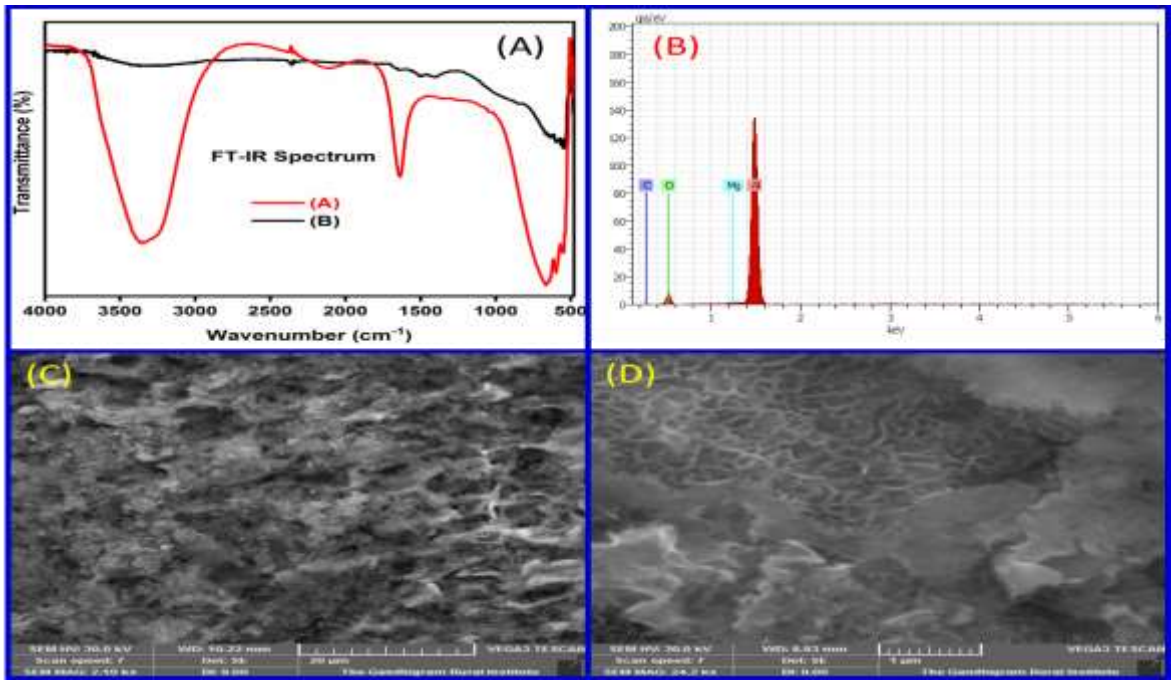

Figure 6 (A) FT-IR spectrum of (a) mixed inhibitor residue (GTLE + AILE), (b) Protective film formed over the AA surface after immersion in the acidic medium at optimum concentration, (B) EDAX spectrum of the AA after treating with mixed inhibitor (GTLE + AILE), SEM micrographs

of (C) uninhibited (D) inhibited AA sample containing mixed inhibitor (GTLE + AILE) extract in acidic medium.

4.5.3. SEM Analysis

Cleaned AA was immersed in the acid solution in the absence and presence of 100 mg/l00ml of mixed inhibitor (GTLE + AILE) for 24 hrs are shown in **Figure 6 (C, D). Figure 6 (C)** shows the surface of AA was hard and strongly damaged in the absence of inhibitors owing to the metal dissolution in an acid solution. The surface was uneven and very porous, and large holes started to show up. After an inhibitor has been added to the solution, a soft and smooth surface can be seen in **Figure 6 (D).** This observation concludes that the CR was reduced in the presence of green mixed inhibitor (GTLE+ AILE) inhibitor which is owing to the adsorption of inhibitor molecules on the metal surface as a protective layer [5].

Table 7. Surface composition (weight %) of AA in absence and presence of mixed inhibitor (GTLE + AILE)

Medium	Elemental composition (%)			
	Al	**O**	**C**	**Mg**
Aluminium Alloy	80.80	41.68	8.72	1.31
Aluminium alloy in mixed inhibitor (GTLE + AILE) solution	71.57	36.91	7.00	0.85

4.6. Mechanism of inhibition

Mixed inhibitor (GTLE + AILE) contain numerous naturally occurring organic compounds. The oxide film that formed on the surface of the aluminium and its alloys can function as a static barrier to separate the metal from the solution. The process by which aluminium dissolves in an acidic solution is as follows: [5].

$$Al + H_2O \rightarrow AlOH + H^+ + e^- \quad (13)$$

$$AlOH_{(ads)} + 5H_2O + H^+ \rightarrow Al^{3+} + 6H_2O + 2e^- \quad (14)$$

$$Al^{3+} + H_2O \rightarrow [AlOH]^{2+} + H^+ \quad (15)$$

$$[AlOH]^{2+} + X^- \rightarrow [AlOHX]^+ \quad (16)$$

The metal dissolves as a result of the formation of a soluble complex ion. The removal of adsorbed water molecules from the metal surface occurs during the displacement reaction that occurs when the inhibitor molecule is adsorbed. The IE of the mixed inhibitor (GTLE + AILE) mainly depends on the presence of active organic compounds in the extract. The extracts on the inhibitor get adsorbed on the metal surface and form a protective film. It restricts the process of diffusion of ions to or from the AA surface and hence retards the corrosion process. The interaction of the metal surface with the inhibitor molecules may prevent the metal atom from activating the anodic

corrosion process. By reducing the number of metal atoms that activate, this blocking effect also reduces the rate of corrosion. The additional inhibitory impact may be brought on by the presence of a hydroxyl group, which can easily form a complex with a trivalent aluminium ion.

4.7 Conclusion

The mixed inhibitor (GTLE + AILE) extract in 1M HCl and 1M H_3PO_4, inhibits the corrosion of AA very well and sustainably. The effectiveness of the inhibition increases with the concentration of the inhibitor and reaches its peak in 1M HCl (97%) and 1M H_3PO_4 (92%) at their optimal concentrations (100 mg/100 mL). IE decreases with the increase in temperature from 303 K to 323 K. The adsorption of mixed inhibitor (GTLE + AILE) on the surface of AA follows Langmuir adsorption isotherm. The mixed inhibitor (GTLE + AILE) extract acts as a mixed-type inhibitor in 1M HCl and 1M H_3PO_4 and the EIS spectra results indicate that the corrosion reaction is controlled by the charge transfer process. The presence of mixed inhibitor (GTLE + AILE) extract in 1M HCl and 1M H_3PO_4 solutions enhances R_{ct} values while reducing C_{dl} values. The introduction of mixed inhibitor (GTLE + AILE) extracts into 1M HCl and 1M H_3PO_4 solution results in the formation of an adsorptive film on the AA surface, which effectively protects the metal from corrosion. The values of ΔG_{ads} are negative, which reveals that the adsorption is a spontaneous process. The Energy of activation value suggests that mixed inhibitor (GTLE + AILE) undergoes physical adsorption on the surface of the aluminium. Protective film formation to prevent the metal from corrosion was confirmed using various spectroscopic and microscopic techniques.

5. References

1. P. R. Kosting, C. Heins, *Ind. Eng. Chem*., **1931**, 23, 140.
2. W. A. Badaway, F. M. AlKharafi, A. S. El-Azab, Corros. Sci., 1999, 41, 709.
3. S. Perumal, S. Muthumanickam, A. Elangovan, R. Sayee kannan, K.K.Mothilal, Int. J. Chemtech Res. 2017, 10 (13), 203-213.
4. E. E. Stansbury, R. A. Buchanan, Fundamentals of Electrochemical Corrosion. ASM International, Materials Park, 2000.
5. J. Jeyasundari, S. Rajendran, R. Sayee Kannan, Y. Brightson Arul Jacob, Eur. Chem. Bull., 2013, 2 (9), 585-591.
6. P. Deepa, R. Padmalatha, J. Environ. Chem. Eng., 2013, 1, 676.
7. M. Hosseni, S. F. L. Mertens, M. Ghorbani, A. R. Arshadi, Mater Chem Phys., 2003, 78, 800.
8. S. Perumal, S. Muthumanickam, A. Elangovan, R. Karthik, R. Sayee Kannan, K. K. Mothilal, J Bio Tribo Corros. 2017, (13) 3, 1-10.
9. A. Popova, M. Chirstov, A. Zwetanova, Corr. Sci., 2007, 49, 2131.
10. M. Sharma, S. B. Prasad, Int. J. Pharmacogn. Phytochem. Res., 2014, 6, 1010.
11. R. Rajagopal, K.V. Kailasam, Pharmacognosy Journal. 2015, 7, 330.
12. S. Perumal, R. Sayee kannan, S. Muthumanickam, A. Elangovan, N. Muniyappan, K. K. Mothilal, J. Adv. Sci. Res., 2022, 13 (3), 151-160.
13. R. Jeevalatha, R. Sayee Kannan, C. Meenakshi, Pramana Research Journal, 2019, 9 (5), 1205-1233.

14. S. Martinez, I. Stern, Appl. Surf. Sci., 2002, 199, 83.
15. A. Popova, E. Okolova, S. Raicheva, M. Christov, Corros. Sci., 2003, 45, 33.
16. D. F. Shriver, P. W. Atkins, C. H. Langford, Inorganic chemistry., 1994, 2, 238.
17. A. K. Singh, M. A. Quraishi, Mater. Chem. Phys., 2010, 123, 666.
18. I. Naqvi, A. R. Saleemi, S. Naveed, Int J Electrochem. Sci., 2011, 6, 146.
19. Avci., Gulsen., Colloids. Surf. A., 2008, 317, 730.
20. Y. B. A. Jacob, R. Sayee Kannan, J. Jeyasundari, Eur. Chem. Bull., 2013, 2 (5), 293-297.
21. A. Y. El-Etre, J Coll Interf. Sci., 2007, 314, 578.
22. M. Behpour, S. M. Ghoreishi, M. Khayatkashani, N. Soltani, Corros. Sci., 2011, 53, 2489.
23. M. Boukalah, B. Hammouti, M. Lagrenee, F. Bentiss, Corros. Sci., 2006, 48, 2831.
24. X. H. Li, S. D. Deng, H. Fu, Prog. Org. Coat., 2010, 67, 420.
25. N. Gunavathy, S. C. Murugavel, E-J. Chem., 2012, 9, 487.
26. U. M. Eduok, S. A. Umoren, A. P. Udoh. Arabian J. Chem., 2012, 5, 325.
27. X. Li, S. Deng, F. Hui, Corr. Sci., 2012, 62, 163.
28. N. Soltani, M. Behpour, H. Ghoreishi, S. M. Naeimi, Corros. Sci., 2010, 52, 1351.
29. M. K. Gomma, M. H. Wahdan, Mater. Chem. Phys., 1995, 39, 209.
30. A. S. Fouda, A. A. Al-Sarawy, E. E. El-Katori, Desalination., 2006, 201, 1.
31. X. Li, S. Deng, F. Hui, T. Li, Electrochim. Acta., 2009, 54, 4089.
32. R. A. Prabhu, T. V. Venkatesha, A. V. Shanbhag, J. Iranian Chem. Soc., 2009, 6, 353.